

1 Meteorological factors driving glacial till variation and the associated
2 periglacial debris flows in Tianmo Valley, southeast Tibetan Plateau

3 M. F. Deng^{1,2}, N. S. Chen^{1*}, and M. Liu^{1,2}

4 (¹Key Laboratory of Mountain Hazards and Surface Process, Institute of Mountain Hazards and Environment,
5 Chinese Academy of Sciences, Chengdu 610041, China;

6 ² University of Chinese Academic of Sciences, Beijing 100049, China)

7 Abstract: Meteorological studies have indicated that high alpine environments are strongly
8 affected by climate warming, and periglacial debris flows are frequent in deglaciated regions. The
9 combination of rainfall and air temperature controls the initiation of periglacial debris flows, and
10 the addition of meltwater due to higher air temperatures enhances the complexity of the triggering
11 mechanism compared to that of storm-induced debris flows. On the southeastern Tibetan Plateau,
12 where temperate glaciers are widely distributed, numerous periglacial debris flows have occurred
13 over the past 100 years, but none occurred in the Tianmo watershed until 2007. In 2007 and 2010,
14 three large-scale debris flows occurred in the Tianmo Valley. In this study, these three debris flow
15 events were chosen to analyse the impacts of the annual meteorological conditions, including the
16 antecedent air temperature and meteorological triggers. TM images and field measurements of
17 the nearby glacier suggested that sharp glacier retreats occurred in the one to two years preceding
18 the events, which coincided with spikes in the mean annual air temperature. Moreover, glacial till
19 changes driven by a prolonged increase in the air temperature are a prerequisite of periglacial
20 debris flows. Different factors can trigger periglacial debris flows, and they may include high
21 intensity rainfall, as in the first and third debris flows, or continuous, long-term increases in air
22 temperature, as in the second debris flow event.

23 Key words: glacial till variation; meteorological factors; periglacial debris flows;
24 southeast Tibetan Plateau

25 **1. Introduction**

26 Alpine environments are vulnerable to climate changes, and alpine glaciers and
27 permafrost are the most sensitive to degradation (Harris et al., 2009; IPCC, 2013).
28 Glacier and permafrost retreat can induce mass movements such as landslides,
29 shallow slides, debris slides, moraine collapses, etc. (Cruden and Hu, 1993; Korup
30 and Clague, 2009; McColl, 2012; Stoffel and Huggel, 2012; Fischer et al., 2012).
31 These movements would bring the material out of the watersheds in the form of debris

32 flows or sediment fluxes. Debris flows in alpine regions often bury residential areas,
33 cut off main roads, block rivers (Shang et al., 2003; Cheng et al., 2005; Deng et al.,
34 2013) and destroy basic facilities downstream; thus, they pose a considerable threat to
35 the local economy and social development. In undeveloped alpine areas where the
36 transportation system is particularly poor or limited, such as in southeastern Tibet, the
37 negative effects produced by debris flows, such as cutting off main roads, can be
38 serious (Cheng et al., 2005).

39 Periglacial debris flows occur in high alpine areas with large areas of glaciers,
40 such as on the Tibetan Plateau in China (Shang et al., 2003; Ge et al., 2014), in the
41 Alps in Europe (Sattler et al., 2011; Stoffel and Huggel, 2012), in the Caucasus
42 Mountains in Russia (Evans et al., 2009) and in northern Canada (Lewkowicz and
43 Harris, 2005). Periglacial debris flows can be initiated by rainfall (Stoffel et al., 2011;
44 Schneuwly-Bollschweiler and Stoffel, 2012), glacial meltwater flow or ice particle
45 ablation (Arenson and Springman, 2005; Decaulne et al., 2005) or outburst floods
46 from glacier lakes (Chiarle et al., 2007) in different parts of the world; however,
47 multiple triggers of a single event have rarely been studied. Because debris flows are
48 commonly triggered by rainfall (Sassa and Wang, 2005; Decaulne et al., 2007; Kean
49 et al., 2013; Takahashi, 2014), the rainfall threshold, intensity and duration have been
50 widely used for debris flow monitoring and to provide event warnings in non-glacier
51 areas (Guzzetti et al., 2008).

52 In deglaciated areas, the debris flow threshold can be more difficult to determine.
53 Periglacial debris flows tend to occur in the summer when the thawing of glaciers and
54 glacial tills predominates and meltwater penetrates the glacial tills at a constant and
55 successive flow rate. The effect of meltwater is similar to that of antecedent rainfall
56 (Rahardjo et al., 2008) and is variable in different periods, considering snow and
57 glacier shrinkage and air temperature fluctuations. In the Swiss Alps, the meltwater
58 volume is high in early summer, and debris flows can be initiated by low intensity
59 rainfall. However, larger rainstorms are required to produce debris flows in late
60 summer and early autumn when the meltwater volume is low (Stoffel et al., 2011;
61 Schneuwly-Bollschweiler and Stoffel, 2012). On the southeastern Tibetan Plateau, the

62 rainfall threshold given by Chen et al. (2011) is relatively wide (0.2~2.0 mm/10min,
63 0.6~6.3 mm/h or 3.0~19.4 mm/24h), the small rainfall threshold of which is likely
64 affected by the air temperature. Moreover, periglacial debris flows induced by sudden
65 releases of water from glacier lakes are closely related to increasing air temperature
66 (Liu et al., 2014).

67 Air temperature fluctuations are likely important triggers of periglacial debris
68 flows. Compared to storm-induced debris flows, increased air temperature can greatly
69 enhance the complexity of the initiation of periglacial debris flows. It is difficult to
70 simulate the triggering process via experiments or mathematical simulation; thus, case
71 studies of natural debris flows must be explored. In this study, three debris flow
72 events in the Tianmo watershed on the southeastern Tibetan Plateau are used as
73 examples after a debris flow-free period of nearly 100 years as deglaciation continues.
74 The annual meteorological conditions, antecedent air temperature and triggering
75 conditions prior to debris flows are analysed to further understand the meteorological
76 triggers and their roles in glacier retreat, glacial till variation and debris flow
77 initiation.

78 **2. Background**

79 **(1) Study area**

80 Temperate glaciers on the Tibetan Plateau are primarily distributed in the Parlung
81 Zangbo Basin, and they covered a total landmass of 2381.47 km² in 2010 based on
82 TM images (taken by the No. 4 or 5 thematic mapper on the Landsat satellite with a
83 spatial resolution of 30 m) (Liu, 2013). Historically, the movement of temperate
84 glaciers has produced numerous moraines, the depth of which can reach 500 m locally
85 (Yuan et al., 2012). In recent decades, a significant temperature increase has
86 occurred, and the temperature at the Bomi meteorological station (central Parlung
87 Zangbo Basin) increased by 0.23°C/10a from 1969 to 2007, resulting in remarkable
88 glacial shrinkage (Yang et al., 2010).

89 Tianmo Valley, which is located in Bomi County and to the south of the

90 ParlungZangbo River, covers an area of 17.76 km² (29°59'N/95°19'E; Figure 1). This
91 valley has a northeast-southeast orientation and is surrounded by high mountains
92 reaching 5590 m a.s.l. at the southernmost location and 2460 m a.s.l. at the fork in the
93 ParlungZangbo River. The TM image from 2013 illustrated the presence of a hanging
94 glacier with an area of 1.42 km² in the upper concave area at an elevation of 4246 m
95 to 4934 m. Bare rock, dipping at an angle of approximately 60°, emerges below and
96 above the hanging glacier and is often covered by snow. Below 3800 ma.s.l.,
97 vegetation, including forest and shrubs, occupies most of the area (Table 1).

98 The river channel in the watershed is sheltered by shade and not directly affected
99 by sunlight, resulting in less solar radiation and a location at which a small trough
100 glacier can form. In the main channel, the trough glacier extended to 2966 m a.s.l. in
101 2006. The lower part of the trough glacier has been eroded by glacier meltwater flow,
102 and an arch glacier that is vulnerable to high pressure was formed (Figure 2). The
103 remnants of the landslide deposits are approximately 10 metres high can be observed
104 on both sides of the channel. These deposits consist of low-stability sediment and can
105 be easily entrained by debris flows.

106 Tianmo Valley is located on the north side of the bend in the YarlungZangbo
107 River and is strongly affected by new tectonic movement. An inferred normal fault
108 vertical to the channel cuts through the valley and is only 30 km from the Yarlung
109 Zangbo fault. In 1950, a rather significant earthquake (Ms. 8.6) hit Zayu, which is
110 only 200 km away, and local records reported that a large amount of rock collapsed
111 and landslides were produced at that time. The whole valley is located in a strong
112 ductile deformation zone and is dominated by gneissic lithology belonging to a
113 Presinian System.

114 **(2) Disaster history**

115 According to our field interviews with local residents, there were no debris flows
116 in the approximately 100 years prior to 2007 in Tianmo Valley. The channel was
117 relatively narrow before 2007, and the local people could walk across via a wooden
118 bridge to live and farm on the terrace on the west side. On the morning of September

119 4th, 2007, after a rainfall even that did not hit the downstream area ceased, the local
120 forest guard heard a loud noise coming from the upstream area at approximately
121 18:00. Rainfall later began in the upstream area at approximately 19:00. Then, debris
122 flows began to occur in the Tianmo Channel, and they subsequently blocked the
123 Parlung Zangbo River. This debris flow event is listed as DF1 in this paper. It is told
124 by the local citizen that several debris flows occurred during that entire night while
125 we cannot separate them. According to the field measurements, approximately
126 1,340,000 m³ of sediment was transported during this event, resulting in 8 missing
127 persons and deaths. Concurrently, debris flows occurred in the four nearby 4 valleys
128 (Table 2). According to the size classification proposed by Jakob (2005), which is
129 based on the total volume, peak discharge and inundated area, the size classes of the
130 debris flows in the five valleys are given in Table 2. At 11:30 on July 25th, 2010,
131 debris flows were again triggered in Tianmo Valley that traced the path of the
132 preceding debris flow deposits and reached the other side of the Parlung Zangbo River.
133 According to Ge et al. (2014), a solid sediment mass of approximately 500,000 m³
134 was carried to (Table 1) and deposited in the channel and blocked the main river. A
135 barrier lake was formed, and the rising water destroyed the roadbed of G318. Dozens
136 of small-magnitude debris flows occurred in the following week. This debris flow
137 event is listed as DF2 in this paper.

138 Debris flows occurred again two months later on Sep. 6th (The Ministry of Land
139 and Resources P. R. C., 2010), although we could not determine the exact time
140 sequence of the events. According to speculation, the debris flows could have occurred
141 in the early morning before dawn when the rainfall intensity reached its maximum
142 (Figure 9). This theory agrees with the findings of Chen (1991), who found that
143 periglacial debris flows historically occurred between 18:00~24:00 in this area. The
144 debris barrier in the main river was consequently increased by an additional 450,000
145 m³, and the barrier lake was enlarged to hold 9,000,000 m³ of water. This debris flow
146 event is listed as DF3 in this paper.

147 A field investigation revealed that a high percentage of boulders in the
148 downstream area and glacial tills above the trough glacier are loose and high porosity

149 rocks (Figure 2); hence, they have low density and can be easily entrained. Our
150 particle size tests of the glacial tills and debris flow deposits indicate a low clay
151 ($d < 0.005$ mm) content, whereas the debris flow deposits contain more fine particles
152 that are smaller than 10 mm (Figure 4), suggesting that entrainment accounted for a
153 considerable amount of fine particles.

154 **(3) Meteorological data**

155 The study area is located in a high alpine area where the economy is relatively
156 undeveloped and few meteorological stations exist. Before 2011, the Bomi
157 meteorological station (established in 1955) was the only station in the area. It is
158 located 54 km from Tianmo Valley at an elevation of 2730 m, and other stations were
159 located more than 200 km away.

160 The Tibetan Plateau is a massive terrace that obstructs the Indian monsoon,
161 causing it to travel through the Yarlung Zangbo Canyon and its tributaries. As the
162 Indian monsoon is transported to higher altitudes, a rainfall gradient emerges in the
163 Parlung Zangbo Basin. However, according to the rainfall data from the area, rainfall
164 often exhibits a similar intensity as that of the long-term rainfall process from
165 Guxiang to Songzong, which suggests that a large rainfall gradient does not exist
166 between Tianmo Valley and Bomi meteorological station; therefore, the rainfall data
167 from Bomi meteorological station could be used in our study. To conduct additional
168 studies, another meteorological station was built in 2011 near Tianmo Valley.

169 It has been established that the air temperature decreases with altitude; therefore,
170 the air temperature in the source area of Tianmo Valley is lower than that in Bomi
171 County. According to the research by Li and Xie (2006), the air temperature decreases
172 at a rate of $0.46\sim 0.69^{\circ}\text{C}/100$ m over the entire Tibetan Plateau, and the rate in the
173 study area is $0.54^{\circ}\text{C}/100$ m. Because the glacier and permafrost in the source area
174 have planar distributions, the air temperature at the geometric centre of the glacier and
175 permafrost can be used to analyse the temperature process.

176 **3. Analysis and results**

177 **(1) Air temperature and rainfall changes**

178 The mean annual air temperature is generally used to reflect the trends of glacier
179 change (Yang et al., 2015). We collected mean annual air temperature and annual
180 rainfall data from 1970 to 2014 from the Bomi meteorological station (Figure 5). The
181 records showed that the mean air temperature has increased by approximately 1.5 °C
182 over the past 45 years at a rate of 0.033 °C/a. This air temperature increase was
183 particularly rapid between 2005 and 2007 at approximately 0.7 °C/3a, which is 7
184 times the average value over the past 45 years. However, the annual rainfall from
185 2000 to 2010 was low and estimated as 828.2 mm per year. From 2000 to 2004, the
186 rainfall during summer (July to September) accounted for approximately 50% of the
187 total annual rainfall; however, only 32% of the rainfall occurred in the summer of
188 2005~2006, even though the annual rainfall exhibited a similar trend. In 2007, rainfall
189 in the summer and the entire year returned to the mean rainfall state.

190 Figure 5 shows similar air temperature and rainfall trends before DF2 and DF3.
191 The air temperature increased in 2009 and reached the maximum temperature over the
192 past 45 years of 10.2 °C; however, the annual rainfall was only 65% of the average
193 amount; and the summer rainfall, which was lower than that in 2005 and 2006,
194 reached a minimum value. In 2010, rainfall was abundant, and the annual rainfall
195 increased to 1080.6 mm, which is approximately 30% more than the average value
196 and close to the maximum.

197 The following common traits can be identified by comparing the annual
198 meteorological conditions of DF1, DF2 and DF3: 1) one or two years before the
199 debris flows, the mean annual temperature increased and the annual rainfall and
200 summer rainfall decreased. Additionally, the climate was in a "hot-dry" state; 2) As
201 the temperature gradually decreased, the annual rainfall returned to normal or
202 increased, and a "hot-wet" climate state contributed to debris flow initiation (Lu and
203 Li, 1989).

204 (2) Changing of glacier in TianmoValley

205 In our study, remote images were collected to analyse the glacier changes in the
206 source area in recent years. To eliminate the effect of snow cover, images were taken
207 in the thawing seasons when snow cover is limited, enabling easy detection of glaciers
208 and snow. Moreover, an image taken on a bright, cloudless day is still needed to show
209 the watershed clearly; however, a difficult case is encountered when the rainy season
210 begins during the thawing season, as the atmosphere is often covered by thick clouds.
211 Furthermore, to illustrate glacier retreat and its impact on debris flows properly, the
212 images should be within similar time intervals, such as 3 years, before and after debris
213 flow events. High-resolution images are rare, and we could only collect one SPOT
214 image (taken by the Systeme Probatoire d'Observation de la Terre satellite with a
215 spatial resolution of 5 m) in 2008. To achieve image consistency, we collected 5 TM
216 images (taken by the No. 4 or 5 thematic mapper on the Landsat satellite with a
217 spatial resolution of 30 m) taken on September 17th, 2000, July 24th, 2003, September
218 21st, 2006, September 24th, 2009 and August 4th, 2013.

219 Based on the 5 TM images, we classified the area as glacier, snow, bare land,
220 gully deposit and vegetation in time series (Figure 6), and the area of each is given in
221 Table 1. Figure 6 shows that deglaciation occurred in Tianmo Valley; notably, the
222 eastern branch has experienced considerable deglaciation. To clearly show the rapid
223 rate of glacial retreat in the entire basin and eastern branch, a graph of retreat was
224 plotted, as shown in Figure 7.

225 Figure 7 shows that the glacier in Tianmo Valley shrank from 2000 to 2013, with
226 variable rates of glacier retreat. In 2000~2003, 2003~2006, 2006~2009 and
227 2009~2013, the glacier retreat rates in Tianmo Valley were 0.02, 0.06, 0.027 and
228 0.0075 km²/a, respectively, and those of the eastern branch were 0.0033, 0.01, 0.008
229 and 0.002 km²/a, respectively. According to the figure, the largest glacier retreat rate
230 was observed in 2003~2006, followed by that in 2006~2009. The glacier area at the
231 beginning should be noted to assess the rate of change of the glacier. The glacier
232 retreat rate can be normalized, and the relative glacier retreat rate can be calculated

233 based on this change in area.

234 The relative glacier retreat rates were 11.30, 35.09, 17.43 and $5.17 \times 10^{-3} \text{ km}^2/\text{a}/\text{km}^2$
235 in 2000~2003, 2003~2006, 2006~2009 and 2009~2013, respectively; and the
236 corresponding values were 20.83, 66.67, 66.67 and $20.83 \times 10^{-3} \text{ km}^2/\text{a}/\text{km}^2$ for the
237 eastern branch. The relative glacier retreat rate of the eastern branch decreased sharply
238 between 2000 ~2013.

239 In this study, TM images over 3-year intervals were applied to obtain the mean
240 glacier retreat rate. As glacier retreat rate in the 3 three years could be either high or
241 low, field measurements of the nearby glacier were used to show the glacier retreat
242 condition before debris flows occurred. Yang et al. (2015) conducted field
243 measurements of the No.94 Glacier in the Parlung Zangbo Basin since 2006, and the
244 field measurements suggest it had a negative balance from 2006~2010 (Figure 7). The
245 negative balance reached a maximum level in 2009, followed by 2008 and 2006,
246 indicating rapid deglaciation in these three years.

247 When we combined the results of the TM image analysis and field measurements
248 of the No. 94 Glacier, we observed that the glacier in Tianmo Valley experienced the
249 most rapid deglaciation prior to debris flows in 2006, 2008 and 2009, which coincided
250 with an increase in the mean annual air temperature (Figure 5). Moreover, the
251 maximum glacier retreat in 2009 was potentially related to the decline in snowfall in
252 the preceding winter and early spring.

253 **(3) Antecedent air temperature and rainfall**

254 The air temperature in the source area can be obtained based on a vertical rate of
255 decline ($0.54 \text{ }^\circ\text{C}/100 \text{ m}$). Based on this method, the air temperature in the source area
256 was $9.8 \text{ }^\circ\text{C}$ lower than that at the Bomi meteorological station. We collected the
257 lowest temperature, the mean temperature and daily rainfall from June to September
258 in 2007 and 2010 (Figure 8).

259 Figure 8 shows that the lowest air temperature was below 0 at the end of June
260 2007. At the beginning of July, the air temperature started to rise quickly, which
261 continued until early September when DF1 occurred. This trend suggests that the high

262 air temperatures in July and August contributed to DF1.

263 Additionally, the air temperature was high from early July to late August, and
264 another high air temperature period was observed in early September. When DF2
265 occurred in late July, the air temperature had reached the maximum for that year,
266 which suggests that the air temperature in early and mid-July was responsible for DF2.
267 After DF2 occurred, the air temperature in August varied towards the conditions that
268 caused DF3.

269 Antecedent air temperature fluctuations include the air temperature and the
270 duration of variations. The air temperatures and durations before debris flows are
271 variable and difficult to evaluate. The accumulation of positive air temperature is
272 often used to analyse the effect of air temperature on glacier melting (Rango and
273 Martinec, 1995) and can be expressed as follows:

$$274 \quad T_{PT} = \sum_{i=-n}^0 T_i (T_i > 0) \quad (1)$$

275 where T_{PT} is positive air temperature accumulation(°C) and T_i is the average
276 daily air temperature(only $T_i > 0$ is included).

277 Because air temperature is successive, it is difficult to determine the beginning of
278 positive air temperature accumulation. Glacial tills can decrease the heat that
279 penetrates into them, and the low air temperature is only observed in the upper thin
280 layer. Moreover, freeze-thaw cycles exist when the lowest air temperature is less than
281 0°C. From this perspective, the beginning of positive air temperature accumulation is
282 defined as the time at which the lowest air temperature exceeds 0°C for two or three
283 successive days or since the last debris flow.

284 Based on the above method, we can deduce that positive air temperature
285 accumulation began when the lowest air temperature exceeded 0°C for several
286 successive days beginning on June 28th, 2007, June 9th, 2010, and July 26th, 2010,
287 which correspond to DF1, DF2 and DF3, respectively. The duration and T_{PT} were
288 calculated for each debris flow event. The results were 69 days and 517.9 °C, 47 days
289 and 332.1 °C and 42 days and 320.4 °C (Figure 8) for DF1, DF2 and DF3,

290 respectively. The results showed that T_{PT} for DF1 was much larger than the other
291 two T_{PT} values, which coincides with the fact that there was no debris flows in the
292 past dozens of years, and extraordinary external forces such as large T_{PT} are required
293 to disrupt the long-term balance.

294 **(4) Triggering conditions**

295 The continuous nature of air temperature limits the possibility for debris flows
296 triggered by a sole abrupt increase in air temperature. Since previous air temperature
297 trends cannot be neglected, it is of no sense to study air temperature triggers.

298 Antecedent rainfall is a factor that favours debris flows. In our analysis, the
299 rainfall over the three days preceding a debris flow event is given in Figure 9.

300 Before DF1, the air temperature was high, which continued through July and
301 August. Notably, the T_{PT} reached 517.9°C. According to the local forest guard, an
302 isolated convective storm occurred prior to DF1, although no rainfall was recorded at
303 the Bomi meteorological station or in the downstream area at that time. In Figure 9, as
304 the rainfall right before DF1 occurred was not recorded by the Bomi metrological
305 station, we added approximately 5 mm/h of rainfall intensity (according to the
306 description provided by the forest guard) before DF1 to account for the storm, which
307 might not reflect the real rainfall process. We can therefore conclude that this isolated
308 convective storm initiated DF1, while the long-term high air temperature trend paved
309 the way for DF1. Considering a large deglaciated area, several other periglacial debris
310 flows simultaneously occurred near Tianmo Valley (Deng et al., 2013), which
311 suggests the advantageous meteorological conditions for debris flow initiation.

312 DF2 occurred when the air temperature reached a peak in 2010. The thaw season
313 began in the middle of June, and T_{PT} reached 332.1 °C. On July 24th, one day before
314 DF2, the air temperature reached a maximum value for that year. The rainfall record at
315 the Bomi meteorological station shows that there had been no rainfall several days
316 preceding DF2, and the local citizens also observed no rain. The trigger of DF2 was

317 likely the continuous percolation of meltwater due to the long-term increase in air
318 temperature.

319 According to field interviews, several debris flows of small magnitude occurred
320 before DF3. The air temperature decreased in late August but increased to another
321 high value before DF3, and the T_{PT} reached 320.4 °C. Rainfall began 2 days prior to
322 DF3 and was steady the entire day before DF3. According to the rainfall trend at the
323 Bomi meteorological station, the rapid increase in rainfall intensity started 4 hours
324 before DF3 and reached 3.8 mm/h, which was responsible for the initiation of DF3.

325 **4. Discussion**

326 In this study, we found that the triggering factors of the three debris flows were
327 high air temperature and rainfall for DF1, high air temperature for DF2 and storm for
328 DF3, respectively. When we analysed the dates and triggers of these events, various
329 questions should be settled first: 1) why did debris flows not occur in 2006 or 2009
330 when deglaciation reached its peak and more ice meltwater was present; 2) why did
331 DF1 and DF3 occur in September when the air temperature and volume of ice
332 meltwater were decreasing; and 3) why were there no large-scale debris flows
333 triggered by previous heavy storms. Based on our results, we believe that the impact
334 of the water source on the magnitude and frequency of debris flows is relatively small,
335 or more debris flows would form during the early larger storm; instead, the soil source,
336 including the associated magnitude and activity, may be the predominant control, as
337 reported by Jakob et al. (2005), who noted that channel recharge is a prerequisite for
338 debris flows. However, in most situations, we cannot reach the source area to detect
339 the soil source, and high-tech remote sensing can only distinguish the boundary of the
340 soil source. In the periglacial area where glacial till is often covered by glacier or
341 everlasting snow, a change in the soil source would be highly difficult to detect. In
342 this study, we combine the meteorological conditions and literature reports to discuss
343 the likely variations in glacial tills before debris flows.

344 **(1) Annual variations in glacial till**

345 Climate warming is a global trend (IPCC, 2013), and the Tibetan Plateau, as the
346 third pole, is no exception to climate change. According to our statistics, the air
347 temperature in Bomi County has increased by 1.5 °C over the past 45 years
348 (1970~2014). Glacier retreat induced by climate warming has been widely accepted,
349 and recent research suggests that the weaker Indian monsoon could be another reason
350 for such retreat (Yao et al., 2012). Glaciers are always located in concave ground
351 areas and cover large volumes of glacial tills. Glacial pressure can generate normal
352 stress vertical to the slope, which can strengthen the slope stability. The effect of
353 glaciers on slope stability is called glacial debuttreasing (Cossart et al., 2008). As
354 deglaciation continues, the result could lead to the exposure of the frozen glacial tills
355 (Figure 10 A to B) and smaller glacial debuttreasing.

356 The retreats of glaciers and glacial tills due to climate warming are quite
357 different. Deglaciation is accompanied by the melting of internal ice particles,
358 which can produce an active surface layer that can obstruct heat fluxes from
359 penetrating into the deep layer and result in the melting of internal ice particles at a
360 rate slower than that of glacial retreat (Takeuchi et al., 2000). Because a strong heat
361 gradient occurs at the surface but is limited in deep layers, glacial tills with thicker
362 coverage always have relatively thinner thawed layers, and the ablation rates of
363 glaciers and internal ice particles are similar to that at the glacier surface and close to
364 the moraine slope. The newly formed bare glacial till is frozen with a high ice
365 content. The cohesion of the ice particles creates a bare glacial till with high shearing
366 strength and stability, and only the surface layer is highly active. Therefore, no debris
367 flows of large magnitude were observed in 2006 and 2009 when glacier retreat
368 reached a maximum and the active glacial till is quite limited.

369 **(2) Variation in glacial till on antecedent days**

370 After the long, cold winter, glacial tills become frozen. If a regressive glacier
371 does not recover in the winter, glacial tills are covered by snow. As the air temperature

372 increases again, the surface snow melts first, followed by the internal ice particles.
373 The thawing of internal ice particles induces a series of changes in the glacial till,
374 which include the following: 1) the thawing will break the bonds of ice particles and
375 increase the instability between ice cracks (Ryzhkin and Petrenko, 1997; Davies et al.,
376 2001); 2) the sharp air temperature fluctuations in high alpine, mountainous areas
377 induce a repeated cycle of expansion and contraction in the glacial till that can destroy
378 the mass structure to some extent; 3) the seepage of ice meltwater can transport
379 fine-grained sediments that were formerly frozen in the ice matrix (Rist, 2007); and 4)
380 the ice meltwater can result in a higher water content and pore water pressure
381 (Christian et al., 2012). These changes in glacial till can sharply decrease the soil
382 strength, shifting to an active mass from an uncovered and frozen moraine (Figure
383 10B to C). Because heat conduction in glacial till is relatively slow, this process may
384 last for a very long time and require a high antecedent air temperature.

385 Heat conduction via the percolation of rainfall and ice meltwater can amplify the
386 depth of active glacial till (Gruber and Haeberli, 2007), whereas covering the surface
387 glacial till can hinder a heat flux from penetrating into the deep layers (Noetzli et al.,
388 2007). At a low air temperature, the heat flux should be constrained to the surface
389 layer, and a large heat gradient due to a high air temperature would contribute much
390 more to the heat flux and ice melt in the deep mass. Thus, the long-term effect of a
391 high air temperature can amplify the active glacial till (Noetzli et al., 2007; Åkerman
392 and Johansson, 2008), under which lies frozen glacial till with a high ice content. The
393 activity of glacial till varies with depth from high at the surface to low in the deep
394 layers, and landslide failure can take place on glacial till slopes in a retrogressive
395 manner, coinciding with long-term air temperature fluctuations, as active glacial till is
396 relatively limited in deglaciated areas.

397 **(3) Failure of glacial till**

398 Different factors can lead to glacial till failure. Active glacial till slopes with low
399 strength are usually vulnerable, and their failure can occur when the air temperature is
400 above 0 °C (Arenson and Springman, 2005). Rainfall or ice melt water induced by air

401 temperature can trigger the failure (Figure 10 C to D). This type of event is called a
402 shallow landslide, and the failure mechanism lies in the ablation of internal ice
403 particles and the percolation of meltwater, which can initially decrease the soil
404 strength (Arenson and Springman, 2005; Decaulne et al., 2005). Later, the subsequent
405 rapid percolation of ice meltwater or heavy rainfall can saturate the debris, decrease
406 soil suction and shearing strength, and form seepage flows that can trigger the shallow
407 landslide failure (Springman et al., 2003; Decaulne and Sæmundsson, 2007; Chiarle et
408 al.,2007). Whether the failure can induce debris flows is still dependent on its ability
409 to entrain the debris layer, in which case the debris is deposited as the flow moves
410 through the channel.

411 Another type of failure might take place when a peaked runoff flows over and
412 entrains debris deposits in the channel and reach a critical discharge (Berti
413 and Simoni, 2005; Gregoretti and Dalla Fontana, 2008; Kean et al., 2013; Takahashi,
414 2014), which is more determined by channel bed slope and grain size of debris
415 (Tognacca et al., 2000; Gregoretti, 2000; Armanini and Gregoretti, 2005; Kean et al.,
416 2013). This type of channelized runoff could be a combination of three factors:
417 rainfall, melting ice or the overflow that forms when a glacier collapses downward
418 into a water pool. Mechanism of this process lies in the hydrodynamic forces, created
419 by the channelized runoff, acting on the surface elements of the debris layer and
420 surpassing resistance of the sediment (Tognacca et al., 2000; Gregoretti, 2000;
421 Armanini and Gregoretti, 2005; Prancevic et al., 2014). The concentration of runoff in
422 the channel bottom causes the erosion of the debris surface layer forming a
423 solid-liquid current at first, then extends to the layers below with whole or partial
424 mobilization and debris flows was generated (Gregoretti and Dalla Fontana, 2008).
425 Therefore, debris flows initiated from seepage flow that leads to a landslide failure or
426 channelized runoff that entrain sediments in the periglacial area is similar with the
427 mechanism of debris flows initiation in non-glacier areas (Iverson et al., 1997;
428 Springman et al., 2003; Sassa and Wang, 2005; Gregoretti and Dalla Fontana, 2008;
429 Kean et al., 2013), while the difference lies in the activity of debris and the source of
430 water. In the European Alps, periglacial debris flows are mainly provoked by rainfall,

431 which is also related to air temperature fluxes (Stoffel et al.,2011). Additionally, the
432 values of rainfall and air temperature required to trigger debris flows could be
433 inversely correlated. Air temperature increases can cause melting and water runoff;
434 thus, the rainfall required to create percolation flows or critical discharge to trigger a
435 debris flow would be much less. In addition, the intensity and duration of the required
436 rainfall may require other preconditions, such as those associated with the
437 distributions of glaciers and frozen glacial tills and the terrain of the source area, to
438 enhance the debris flow (Lewkowicz and Harris, 2005).

439 The three debris flow events were associated with similar annual meteorological
440 conditions, except that the positive air temperature accumulation prior to DF1 was
441 largest. DF1 occurred at the end of a prolonged period of high air temperature, prior to
442 this, there were instances of failure but no large-scale debris flows. On July 25th, 2010,
443 when the daily rainfall reached 20.7 mm, no debris flows were generated because
444 thick active glacial till was still lacking after small failure events. In 2010, the largest
445 daily rainfall occurred on June 7th, accounting for 37.5 mm, at the beginning of an air
446 temperature increase when the glacial till was frozen and had low activity. The lack of
447 glacial till activity was the likely cause of the absence of debris flows. On August 23rd,
448 the daily rainfall was 20.3 mm, the antecedent air temperature accumulation had
449 remained stable since DF2 and active glacial till was still developing. On September
450 6th, the antecedent positive air temperature accumulation was small, and a low air
451 temperature was observed previously; however, the high rainfall intensity
452 supplemented this lack of prolonged high air temperature.

453 **5. Conclusion**

454 Climate changes have serious effects in high mountainous areas, and the mass
455 movement of sediments such as periglacial debris flows has become increasingly
456 frequent. Prolonged increases in the mean annual air temperature are regarded as very
457 favourable for periglacial debris flows. In particular, the annual “hot-dry” weather
458 conditions one or two years prior were responsible for three debris flow events in
459 Tianmo Valley. Debris flows are generally not initiated in the year when the mean

460 annual air temperature spikes, as the melting of internal ice particles lags behind the
461 rate of glacial retreat resulting from a prolonged increase in air temperature.

462 Glacial till is unlimited in deglaciated areas, and its activity relies on glacial
463 retreat and internal ice particle melting. Glacial till changes induced by increased air
464 temperature are the first steps in forming periglacial debris flows compared
465 to storm-induced debris flows in non-glacier areas. Glacial tills require a four-phase
466 process prior to debris flow occurrence. In this process, the variable air temperature
467 condition due to different factors drives the glacial till changes, and temperature
468 increases can cause glacier recession, produce bare glacial till and enhance the glacial
469 till activity. Debris flows can occur when a sufficient amount of active glacial till
470 exists and rainfall-induced seepage or runoff is more likely to generate debris flows.

471 It is difficult to observe glacial till changes in source areas of debris flows, and
472 the analysis of the phase conversion of glacial till in this study is based on the
473 triggering conditions and other literature findings. Indeed, the meteorological
474 conditions, such as the antecedent air temperature and meteorological triggers that
475 drive the phase conversion, are partly coupled and difficult to distinguish. In
476 future studies, we hope to determine the effect of each meteorological condition, and
477 more detailed studies should be performed.

478 **Acknowledgements:** This research was supported by the National Natural Science Foundation
479 of China (grant nos. 41190084, 41402283 and 41371038) and the “135” project of IMHE, CAS.
480 We wish to acknowledge the editors of the Natural Hazards and Earth System Science Editorial
481 Office and the anonymous reviewers for their constructive comments, which helped us improve
482 the contents and presentation of the manuscript.

483 **References**

484 Åkerman, H. J. and Johansson, M.: Thawing permafrost and thicker active layers in
485 sub-Arctic Sweden, *Permafrost Periglac. Process.*, 19, 279-292, 2008.

486 Arenson, L. U. and Springman, S. M.: Mathematical descriptions for the behaviour of
487 ice-rich frozen soils at temperatures close to 0 °C, *Can. Geotech. J.*, 42, 431-442,
488 2005.

489 Armanini, A., and Gregoretti, C.: Incipient sediment motion at high slopes in uniform
490 flow condition. *Water Res Res.*, 41: W12431, 2005.

491 Berti, M., and Simoni, A.: Experimental evidences and numerical modelling of debris
492 flow initiated by channel runoff. *Landslides*, 2(3), 171-182, 2005.

493 Bommer, C., Fitze, P. and Schneider, H.: Thaw-consolidation effects on the stability
494 of Alpine talus slopes in permafrost, *Permafrost Periglac. Process.*, 23, 267-276,
495 2012. doi:10.1002/ppp.1751.

496 Chen, N. S., Zhou, H. B., and Hu, G. S.: Development rules of debris flow under the
497 influence of climate change in Nyingchi, *Adv. Clim. Change Res.*, 7, 412-417,
498 2011. (In Chinese).

499 Chen, R.: Initiation and the Critical Condition of Glacial Debris Flow, Master thesis,
500 Institute of Mountain Hazards and Environment, Chinese Academic of Sciences,
501 P19, 1991.

502 Cheng, Z. L., Wu, J. S., and Geng, X.: Debris flow dam formation in southeast Tibet,
503 *J. Mt Sci.*, 2, 155-163, 2005.

504 Chiarle, M., Iannotti, S., Mortara, G., and Deline, P.: Recent debris flow occurrences
505 associated with glaciers in the Alps, *Glob. Planet. Change*, 56, 123-136, 2007.

506 Cossart, E., Braucher, R., Fort, M., Bourlès, D. L., and Carcaillet, J.: Slope instability
507 in relation to glacial debuitressing in alpine areas (Upper Durance catchment,
508 southeastern France): evidence from field data and ¹⁰Be cosmic ray exposure
509 ages, *Geomorphology*, 95, 3-26, 2008.

510 Cruden, D. M. and Hu, X. Q.: Exhaustion and steady state models for predicting
511 landslide hazards in the Canadian Rocky mountains, *Geomorphology*, 8,
512 279-285, 1993.

513 Davies, M. C. R., Hamza, O., and Harris, C.: The effect of rise in mean annual
514 temperature on the stability of rock slopes containing ice-filled discontinuities,
515 *Permafrost Periglac. Process.*, 12, 137-144, 2001.

516 Decaulne, A. and Sæmundsson, T.: Spatial and temporal diversity for debris-flow
517 meteorological control in subarctic oceanic periglacial environments in Iceland,
518 Earth Surf. Process. Landf., 32, 1971–1983, 2007. doi:10.1002/esp.1509.

519 Decaulne, A., Sæmundsson, T., and Petursson, O.: Debris flows triggered by rapid
520 snowmelt in the Gleidarhjalli area, northwestern Iceland, Geografiska Annaler,
521 87A, 487-500, 2005 .

522 Deng, M. F., Chen, N. S., Ding, H. T., and Zhou, C. C.: The hydrothermal condition
523 of 2007 group-occurring debris flows and its triggering mechanism in Southeast
524 Tibet, J. Nat. Dis., 22, 128-134, 2013 (In Chinese).

525 Evans, S. G., Tutubalina, O. V., Drobyshev, V. N., Chernomorets, S. S., McDougall,
526 S., Petrakov, D. A., and Hungr, O.: Catastrophic detachment and high-velocity
527 long-runout flow of Kolka Glacier, Caucasus Mountains, Russia in 2002,
528 Geomorphology, 105, 314-321, 2009.

529 Fischer, L., Purves, R. S., Huggel, C., Noetzli, J., and Haeberli, W.: On the influence
530 of topographic, geological and cryospheric factors on rock avalanches and
531 rockfalls in high-mountain areas, Nat. Hazards Earth Syst. Sci., 12, 241-254,
532 2012.

533 Ge, Y. G., Cui, P., Su, F. H., Zhang, J. Q., and Chen, X. Z.: Case history of the
534 disastrous debris flows of Tianmo watershed in Bomi County, Tibet, China:
535 some mitigation suggestions, J. Mtn. Sci., 11, 1253-1265, 2014.

536 Gregoretti, C., and Dalla Fontana, G.: The triggering of debris flow due to
537 channel-bed failure in some alpine headwater basins of the Dolomites: analyses
538 of critical runoff, Hydrol. Process., 22, 2248-2263, 2008.

539 Gregoretti, C.: The initiation of debris flow at high slopes: experimental results, J.
540 Hydraulic Res., 38, 83-88, 2000.

541 Gruber, S., and Haeberli, W.: Permafrost in steep bedrock slopes and its
542 temperature-related destabilization following climate change. J. Geophys. Res.,
543 112, (F02S18), 2007.

544 Guzzetti, F., Peruccacci, S., Rossi, M., and Stark, C. P.: The rainfall
545 intensity–duration control of shallow landslides and debris flows: an update,
546 *Landslides*, 5, 3-17, 2008.

547 Harris, C., Arenson, L. U., Christiansen, H. H., Etzelmüller, B., Frauenfelder, R.,
548 Gruber, S., Haeberli, W., Hauck, C., Hölzle, M., Humlum, O., Isaksen, K., Kääb,
549 A., Kern-Lütschg, M. A., Lehning, M., Matsuoka, N., Murton, J. B., Nötzli, J.,
550 Phillips, M., Ross, N., Seppälä, M., Springman, S. M., and Vonder Mühll, D.:
551 Permafrost and climate in Europe: monitoring and modelling thermal,
552 geomorphological and geotechnical responses, *Earth Sci. Rev.*, 92, 117-171,
553 2009.

554 Intergovernmental Panel of Climate Change, Summary for Policymakers. Working
555 Group I Contribution to the IPCC Fifth Assessment Report Climate Change
556 2013: The Physical Science Basis, Cambridge University Press, Cambridge, UK,
557 2013.

558 Iverson, R. M., Reid, M. E., and LaHusen, R. G., Debris-flow mobilization from
559 landslides, *Annu. Rev. Earth Planet Sci.*, 25, 85-138, 1997.

560 Jakob, M., Bovis, M., and Oden, M.: The significance of channel recharge rates for
561 estimating debris-flow magnitude and frequency, *Earth Surf. Proc. Land*, 30,
562 755-766, 2005.

563 Jakob, M.: A size classification for debris flows, *Eng. Geol.*, 79, 151-161, 2005.

564 Kean, J. W., McCoy, S. W., Tucker, G. E., Staley, D. M., and Coe, J. A.:
565 Runoff-generated debris flows: observations and modeling of surge initiation,
566 magnitude, and frequency, *J. Geophys. Res. Earth Surf.*, 118, 2190-2207, 2013.

567 Korup, O. and Clague, J. J.: Natural hazards, extreme events, and mountain
568 topography, *Quat. Sci. Rev.*, 28, 977-990, 2009.

569 Lewkowicz, A. G. and Harris, C.: Frequency and magnitude of active-layer
570 detachment failures in discontinuous and continuous permafrost, northern
571 Canada, *Permafrost Periglac. Process.*, 16, 115-130, 2005.

572 Li, Q. Y. and Xie, Z. C.: Analysis on the characteristics of the vertical lapse rates of
573 temperature. Taking Tibetan Plateau and its adjacent area as an example, *J*
574 *Shihezi University (Natural Science)*, 24, 719-723, 2006 (In Chinese).

575 Liu, J. J., Cheng, Z. L., and Su, P. C.: The relationship between air temperature
576 fluctuation and Glacial Lake outburst floods in Tibet, China, *Quat. Int.*, 321,
577 78-87, 2014.

578 Liu, Y.: Research on the Typical Debris Flows Chain Based On RS in Palongzangbu
579 Basin of Tibet, Master thesis, Chengdu University of Science And Technology,
580 2013 (In Chinese).

581 Lu, R.R. and Li, D.J.: Ice-snow-melt debris flows in the Dongru Longba, Bomi
582 county, Xizang, *J. Glaciol. Geocryol.*, 11, 148-160, 1989. (In Chinese).

583 McColl, S. T.: Paraglacial rock-slope stability, *Geomorphology*, 153–154, 1-16, 2012.

584 Noetzli, J., Gruber, S., Kohl, T., Salzmann, N., and Haerberli, W.: Three-dimensional
585 distribution and evolution of permafrost temperatures in idealized
586 high-mountain topography, *J. Geophys. Res.*, 112, F02S13, 2007.

587 Prancevic, J. P., Lamb, M. P., and Fuller, B. M.: Incipient sediment motion across the
588 river to debris-flow transition. *Geology*, 42(3), 191-194, 2014.

589 Rahardjo, H., Leong, E. C., and Rezaur, R. B.: Effect of antecedent rainfall on
590 pore-water pressure distribution characteristics in residual soil slopes under
591 tropical rainfall, *Hydrol. Process.*, 22, 506-523, 2008.

592 Rango, A. and Martinec, J.: Revisiting the degree-day method for snowmelt
593 computations, *JAWRA, J. Am. Water Resour. Assoc.*, 31, 657-669, 1995.

594 Rist, A.: Hydrothermal Processes within the Active Layer above Alpine Permafrost in
595 Steep Scree Slopes and Their Influence on Slope Stability, PhD Thesis, Swiss
596 Federal Institute for Snow and Avalanche Research and University of Zurich,
597 168 pp., 2007.

598 Ryzhkin, I. A. and Petrenko, V. F.: Physical mechanisms responsible for ice adhesion,
599 *J. Phys. Chem. B*, 101, 6267-6270, 1997.

600 Sassa, K. and Wang, G. H., Mechanism of Landslide-Triggered Debris Flows:
601 Liquefaction Phenomena due to the Undrained Loading of Torrent Deposits.

602 Debris-flow Hazards and Related Phenomena, Springer, Berlin Heidelberg,
603 81-104, 2005.

604 Sattler, K., Keiler, M., Zischg, A., and Schrott, L.: On the connection between debris
605 flow activity and permafrost degradation: a case study from the Schnalstal,
606 South Tyrolean Alps, Italy, *Permafrost Periglac. Process.*, 22, 254-265, 2011.

607 Schneuwly-Bollschweiler, M. and Stoffel, M.: Hydrometeorological triggers of
608 periglacial debris flows in the Zermatt valley (Switzerland) since 1864, *J.*
609 *Geophys. Res.*, 117, F02033, 2012.

610 Shang, Y. J., Yang, Z. F., Li, L., Liu, D. A., Liao, Q., and Wang, Y.: A super-large
611 landslide in Tibet in 2000: background, occurrence, disaster, and origin,
612 *Geomorphology*, 54, 225-243, 2003.

613 Springman, S. M., Jommi, C., and Teyssere, P.: Instabilities on moraine slopes
614 induced by loss of suction: a case history, *Géotechnique*, 53, 3-10, 2003.

615 Stoffel, M. and Huggel, C.: Effects of climate change on mass movements in
616 mountain environments, *Prog. Phys. Geog.*, 36, 421-439, 2012.

617 Stoffel, M., Bollschweiler, M., and Beniston, M.: Rainfall characteristics for
618 periglacial debris flows in the Swiss Alps: past incidences–potential future
619 evolutions, *Clim. Change*, 105, 263-280, 2011.

620 Takahashi, T., *Debris Flow: Mechanics, Prediction and Countermeasures*, CRC Press,
621 Boca Raton, FL, 2014.

622 Takeuchi, Y., Kayastha, R. B., and Nakawo, M.: Characteristics of ablation and heat
623 balance in debris-free and debris-covered areas on Khumbu Glacier, Nepal
624 Himalayas, in the pre-monsoon season. *IAHS PUBLICATION*, 53-62, 2000.

625 The Ministry of Land and Resources P. R. C.: *China geological hazard*
626 *Bulletin*(September edition), 2010.

627 Tognacca, C., Bezzola, G. R., and Minor, H. E.: Threshold criterion for debris-flow
628 initiation due to channel bed failure, in: *Wieczoreck, G. F. (Ed.), Proceedings*
629 *Second International Conference on Debris Flow Hazards Mitigation,*
630 *Prediction and Assessment*, Taipei, 89-97, 2000.

- 631 Yang, W., Guo, X., Yao, T., Zhu, M. and Wang, Y.: Recent accelerating mass loss of
632 southeast Tibetan glaciers and the relationship with changes in macroscale
633 atmospheric circulations, *Clim. Dynam.*, 47, 805–815, 2016.
- 634 Yang, W., Yao, T., Xu, B., Ma, L., Wang, Z., and Wan, M.: Characteristics of recent
635 temperate glacier fluctuations in the Parlung Zangbo River basin, southeast
636 Tibetan Plateau, *Chin. Sci. Bull.*, 55, 2097-2102, 2010.
- 637 Yao, T.D., Thompson, L., Yang, W., Yu, W., Gao, Y., Guo, X., Yang, X., Duan, K.,
638 Zhao, H., Xu, B., Pu, J., Lu, A., Xiang, Y., Kattel, D.B., and Joswiak, D.:
639 Different glacier status with atmospheric circulations in Tibetan Plateau and
640 surroundings, *Nat. Clim. Change*, 2, 663-667, 2012.
- 641 Yuan, G.X., Ding, R.W., Shang, Y.J., and Zeng, Q.L.: Genesis of the Quaternary
642 accumulations along the Palong section of the Sichuan-Tibet Highway and
643 Their distribution regularities, *Geology and Exploration*, 48, 170-176, 2012 (In
644 Chinese).
- 645

646

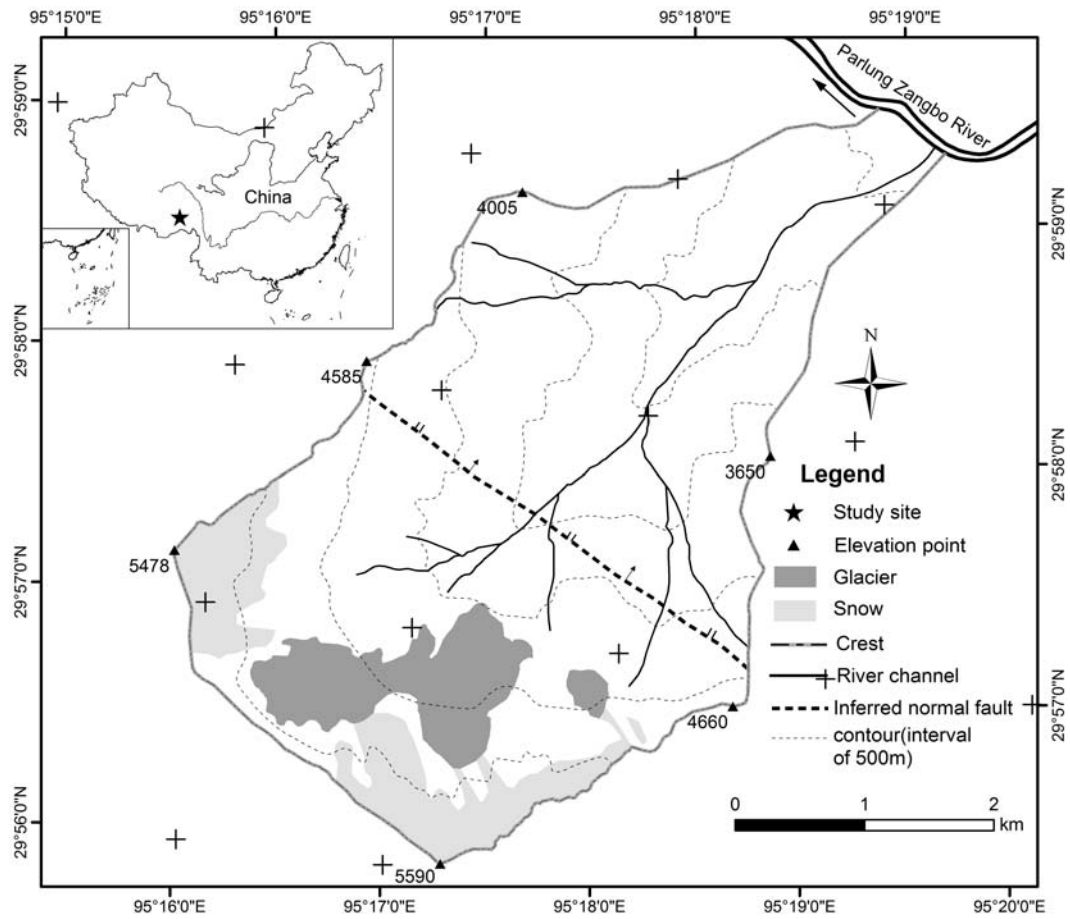
647 Table 1 Changes in glacier, snow, bare land, gully deposition and vegetation in Tianmo Valley

Year	Glacier (km ²)	Glacier(eastern branch) (km ²)	Snow (km ²)	Bare land (km ²)	Gully deposition (km ²)	Vegetation (km ²)
2000	1.77	0.16	2.13	2.80	0.44	10.46
2003	1.71	0.15	2.44	2.54	0.44	10.48
2006	1.53	0.12	2.68	2.44	0.44	10.55
2009	1.45	0.096	2.81	3.03	0.47	9.90
2013	1.42	0.088	1.74	3.83	0.51	10.17

648

649 Table 2 Basic information regarding the debris flows in Tianmo Valley and nearby valleys

No.	Name	Coordinates	Basin area (km ²)	Glacier area (in 2006) (km ²)	Date	Size class
1	Tianmo Valley	29°59'N 95°19'E	17.74	1.53	4 th Sep. 2007	6
					25 th Jul. 2010	5
					6 th Sep. 2010	5
2	Kangbu Valley	30°16'N 94°48'E	48.7	1.06	4 th Sep. 2007	3
3	Xuewa Valley	29°57'N 95°23'E	33.22	0.95	4 th Sep. 2007	2
4	Baka Valley	29°53'N 95°33'E	22.15	2.46	7 th Sep. 2007	3
5	Jiaqing Valley	30°16'N 94°49'E	15.51	1.12	9 th Sep. 2007	3



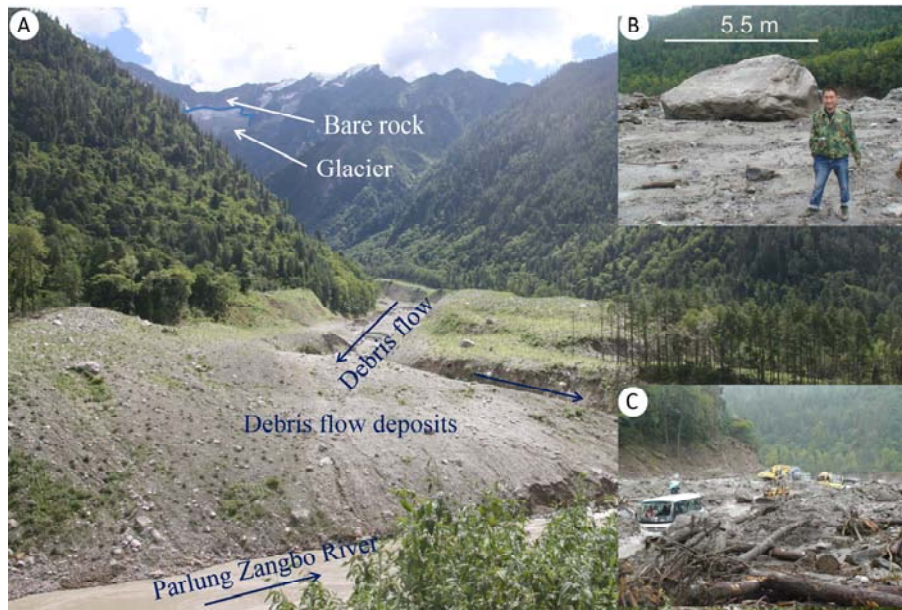
650
651

Figure 1 Location of Tianmo Valley and related information



652
653

Figure 2 Overview of the valley from the channel(in 2014)

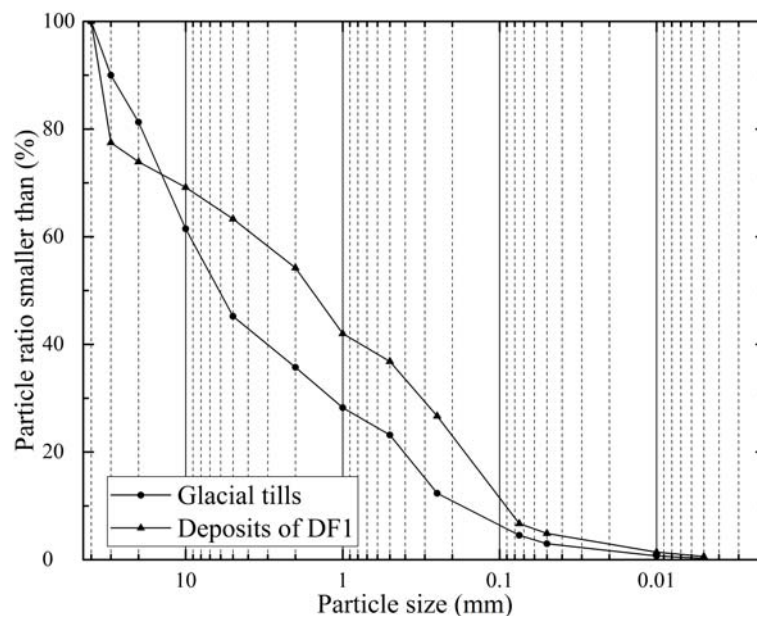


654

655 Figure 3 DF1 in 2007(A. Overview of the Tianmo debris flows from the downstream area; B& C.

656

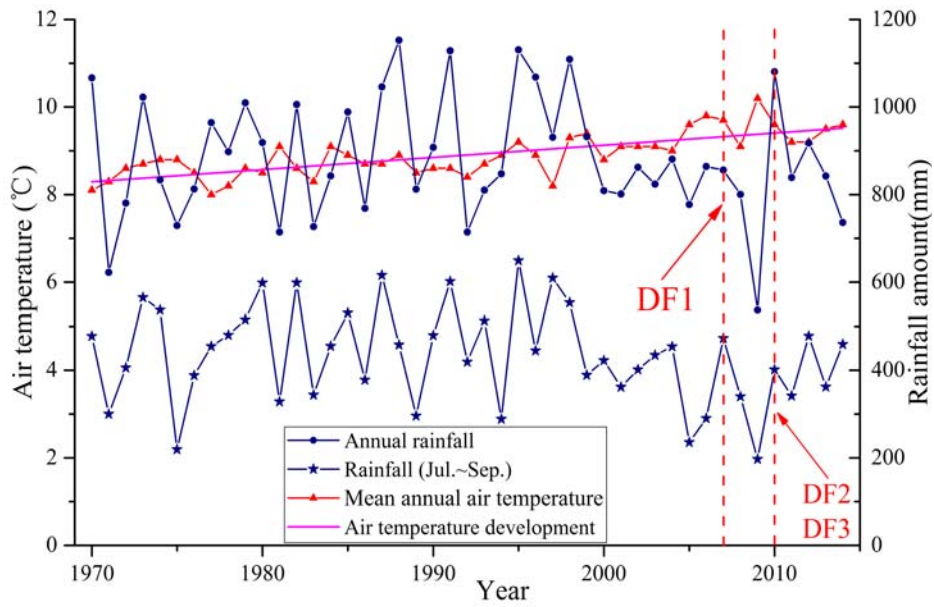
Boulder and debris flow deposits on the north side of the Parlung Zangbo River)



657

658

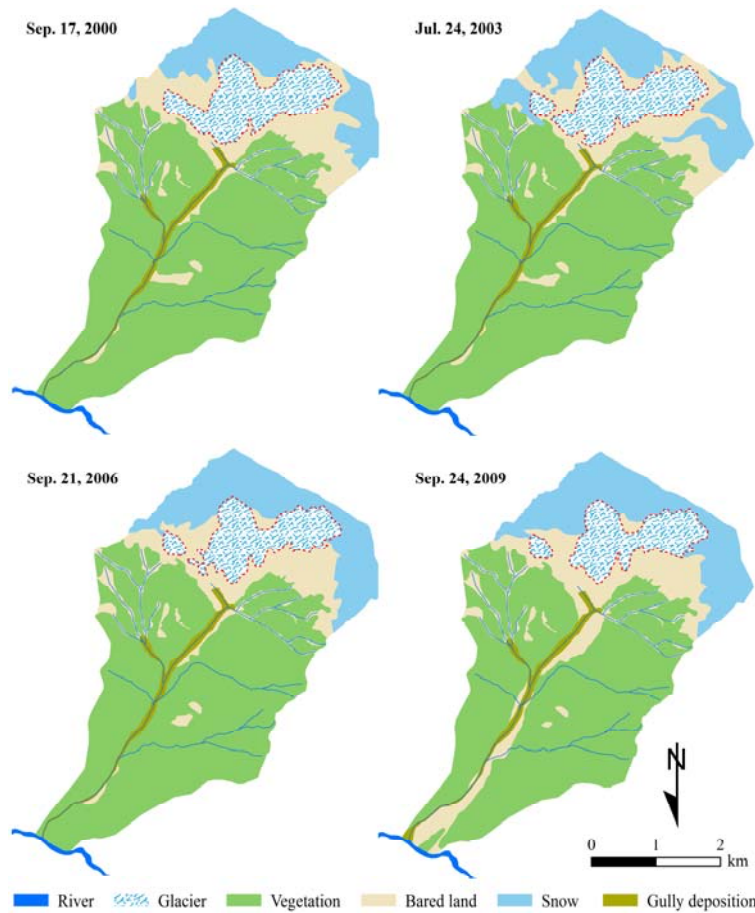
Figure 4 Particle size distributions of the glacial tills and debris flow deposits



659

660

Figure 5 Variation in the mean annual air temperature and rainfall at Bomi from 1970 to 2014



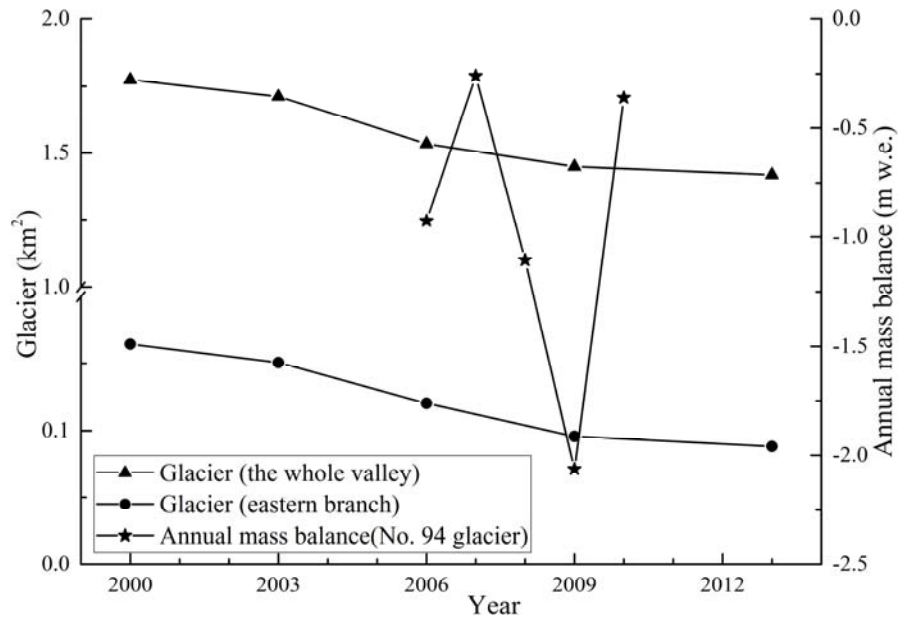
661

662

663

664

Figure 6 Distribution and changes in glacier, snow, bare land, gully deposition and vegetation in Tianmo Valley



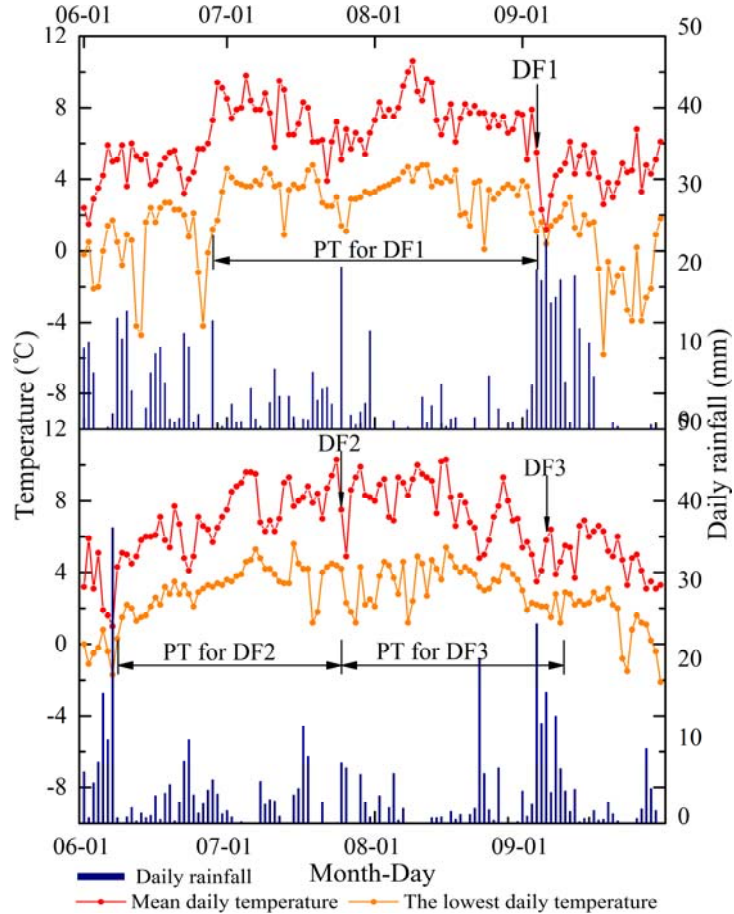
665

666

667

Figure 7 Changes in glacier over time and the measured annual mass balance of the Parlung No.

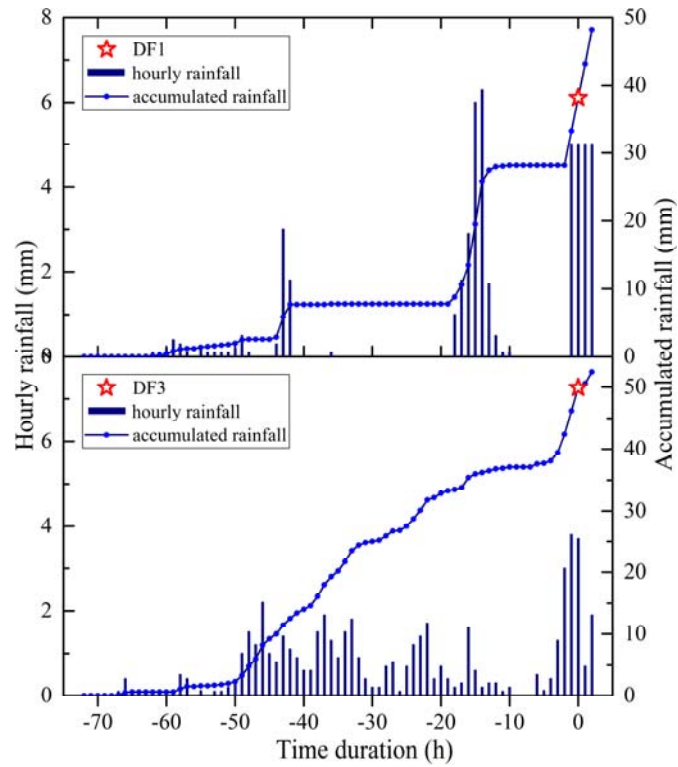
94 Glacier (mass balance was edited from Yang et al.(2015))



668

669

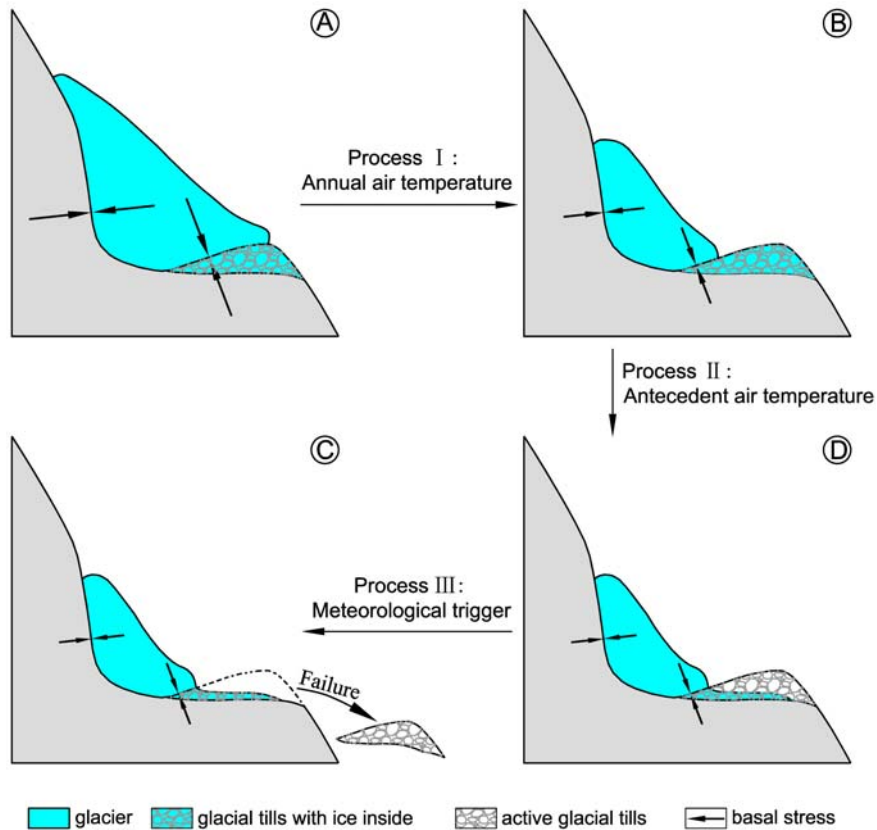
Figure 8 Air temperature and rainfall before and after DF1, DF2 and DF3



670

671

Figure 9 Variations in rainfall accumulation prior to DF1 and DF3 (no rainfall before DF2)



672

673

674

675

Figure 10 Changes in glacier and frozen glacial till before periglacial debris flow initiation (A: glacial-covered glacial tills; B: uncovered and frozen glacial tills; C: active glacial tills; D: failure of glacial tills)